Catalysis Communications 18 (2012) 51–54

Contents lists available at SciVerse ScienceDirect

Catalysis Communications

journal homepage: www.elsevier.com/locate/catcom

Short Communication

Highly active Pt–Ru nanowire network catalysts for the methanol oxidation reaction

Bing Li [a,b], Drew C. Higgins [b], Shaomin Zhu [b], Hui Li [c], Haijiang Wang [c], Jianxin Ma [a], Zhongwei Chen [b,*]

[a] School of Automotive Studies, 4800 Caoan Road, Tongji University, Shanghai 201804, China
[b] Department of Chemical Engineering, Waterloo Institute for Nanotechnology, University of Waterloo, Waterloo, Ontario, Canada N2L 3 G1
[c] Institute for Fuel Cell Innovation, National Research Council Canada 4250 Wesbrook Mall, Vancouver, B. C., Canada V6T 1 W5

ARTICLE INFO

Article history:
Received 11 October 2011
Received in revised form 4 November 2011
Accepted 10 November 2011
Available online 20 November 2011

Keywords:
DMFC
Nanowire networks
Pt–Ru
Methanol oxidation reaction
Electrocatalyst

ABSTRACT

Platinum–ruthenium alloy nanowire networks (Pt–Ru NWNs) have been successfully synthesized by a surfactant assisted soft template strategy, involving the chemical reduction of platinum and ruthenium complexes using sodium borohydride. These materials are investigated as methanol oxidation reaction (MOR) catalysts for fuel cell applications and were found to display exemplary MOR activity and CO tolerance through cyclic voltammetry (CV) testing. Pt–Ru-NWNs investigated in this work are proposed as promising anode replacements to traditional Pt–Ru catalysts in direct methanol fuel cells.

1. Introduction

Direct methanol fuel cells (DMFCs) are promising devices for portable power and transportation applications due to their high energy densities, low emissions, and facile fuel distribution and storage [1]. However, several challenges still face the commercialization of DMFCs. This includes the high system cost arising from the heavy reliance on expensive Pt-based catalyst materials, performance challenges stemming from the sluggish methanol oxidation reaction (MOR) and oxygen reduction reaction (ORR) kinetics [2], along with catalyst poisoning issues by CO species [3]. More specifically, the MOR occurring on platinum, or platinum-based anode catalysts is a self poisoning reaction. Strongly adsorbed CO intermediates are formed by the dehydrogenation of methanol, blocking the catalyst surface for further methanol adsorption and leading to diminished DMFC power densities [4]. Thus, it is of significant interest to develop new anode catalysts that can effectively enhance the methanol electro-oxidation kinetics and tolerance toward CO poisoning, a crucial challenge facing the sustainable commercialization of DMFCs.

In recent years, numerous strategies have been employed in an attempt to improve the performance of MOR catalysts, by developing materials with improved utilization, mass transport properties, operational stabilities and alleviated CO poisoning [5]. Moreover, reducing the system cost of DMFCs by alleviating the extensive reliance on catalysts with a high Pt content is essential. Significant research efforts have been carried out in pursuit of these goals with a focus on either alloying Pt catalysts with a second element, or through deliberate nanostructure control in order to improve the Pt-mass based activities of these materials [6,7]. Alloying with Ru has shown the most promise with respect to MOR catalyst materials, as Ru has been shown to improve catalytic activities due to enhanced electronic properties and lattice contraction, along with improved oxidation of adsorbed CO species. Generally, Pt–Ru black is considered the best performing electrocatalyst, however recent reports have investigated nanostructure control strategies in order to improve MOR activity. Koczkur et al. [8] developed nanoporous Pt–Ru networks utilizing Ti substrates and Choi et al. [9] developed Pt–Ru nanowire networks using SBA-15 templates, both of which displayed promising performance as MOR electrocatalyst materials. These materials are however developed by hard-template and substrate based synthesis procedures. This results in complex multi-step synthesis procedures, requiring harsh chemical treatments (i.e. HF) to remove the templates, and results in networks with low interconnectivity [10].

In the present work, we report the fabrication of Pt–Ru alloy nanowire networks (Pt–Ru NWNs) using a surfactant-assisted soft template (cetyltrimethylammonium bromide, CTAB) synthesis procedure. This surfactant based soft template synthesis method is simplistic and provides flexibility in the design and control of Pt-based alloy nanostructures compared to hard-template approaches. Pt–Ru NWNs can serve to enhance mass transport, electron transport, electrocatalytic activity, utilization and durability due to their distinct morphology and structural properties. Moreover, Pt modified by Ru (alloying) leads to lattice contraction and enhanced electronic properties which can also serve to improve electrocatalytic activity and chemical

* Corresponding author. Fax: +1 519 746 4979.
E-mail address: zhwchen@uwaterloo.ca (Z. Chen).

1566-7367/$ – see front matter © 2011 Elsevier B.V. All rights reserved.
doi:10.1016/j.catcom.2011.11.018

stability. Thus, Pt–Ru NWNs developed using a soft surfactant-assisted synthesis procedure are presented as highly active MOR electrocatalyst materials for the first time.

2. Experimental

2.1. Pt–Ru NWNs synthesis

In a typical synthesis, a mixture of H_2PtCl_6 (5 mL, 20 mM) and $RuCl_3$ (5 mL, 20 mM) aqueous solutions was mixed with 10 mL of chloroform containing 40 mM CTAB under stirring. Stirring was maintained for 60 min, followed by the addition of 80 mL of DDI water. After stirring for 30 min, 0.2 g of sodium borohydride dissolved in 10 mL of pure water was added into the flask while stirring at a speed of 1000 rpm for 20 min. The mixture immediately turned into a dark gray color, indicating the formation of metallic nanocrystals [10]. The resulting solution was filtered and the powder was washed with ethanol and dried at 60 °C for 2 h. In order to optimize the obtained nanostructures in pursuit of highly active Pt–Ru catalysts, we have considered how synthesis conditions may affect the resulting products. The amount of reducing agent and the atomic ratio of Pt and Ru in the precursor solutions utilized can both potentially affect the nanostructure and electrocatalytic activity of these Pt–Ru catalysts, parameters that are investigated herein.

2.2. Material characterization

X-ray diffraction patterns (XRD) were obtained to investigate the Pt–Ru crystalline phases present in the Pt–Ru alloy, utilizing an x-ray wavelength of 1.54 Å. The working voltage was 40 kV, and the current was 40 mA. The intensity data were collected at 25 °C in a 2θ range of 30°–100° with a scan rate of 0.05° min^{-1}. The microstructural parameters of samples were determined using JADE5 software. The morphology of Pt–Ru catalysts was observed using a JEOL 2010F transmission electron microscope (TEM) operating at 200 kV and equipped with energy dispersive spectroscopy (EDS) capabilities.

2.3. Electrochemical testing

For electrochemical testing, 4 mg of Pt–Ru NWN catalysts was suspended in 2 mL of an ethanol/water/Nafion solvent to prepare a catalyst ink. Then, 10 μL of the ink was deposited onto a glassy carbon working disk electrode twice. Pt–Ru NWNs were tested for their electrochemical MOR activity in a glass cell consisting of a three-electrode system in 1 M methanol + 0.1 M $HClO_4$ electrolyte at 25 °C. A Ag/AgCl was used as the reference electrode, and a platinum wire was used as the counter electrode. Commercial Pt black, 20% Pt/C and Pt–Ru black (BASF Fuel Cell, Inc) were also tested for comparison. Cyclic voltammetry (CV) was carried out by six repeated cycles between −0.28 and 0.96 V vs Ag/AgCl at a scan rate of 5 mV s^{-1}.

3. Results and discussion

3.1. Material characterization

Fig. 1 presents the XRD patterns of Pt NWN and Pt–Ru NWN catalysts prepared with different amounts of reducing agent. Namely, Pt–Ru NWN catalysts synthesized using 0.2 g, 0.4 g and 0.6 g of reducing agent are referred to as Pt–Ru 0.2 g, Pt–Ru 0.4 g and Pt–Ru 0.6 g, respectively. From Fig. 1, the typical characteristic reflections of Pt can be seen clearly, corresponding to the face-centered cubic crystalline structure of Pt. After the incorporation of ruthenium, broadened Pt peaks were observed with reduced intensity. In addition, the Pt (220) peak positions located at ca. 67° shifted to higher diffraction angles, in comparison with those from pure Pt NWNs. This indicates contraction of the lattice due to the incorporation of Ru atoms [11].

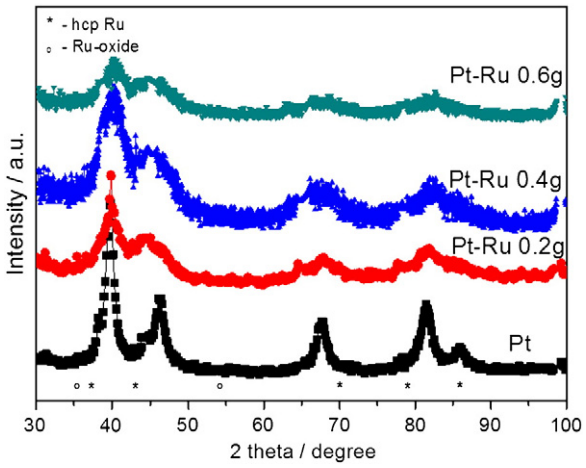

Fig.1. XRD patterns of Pt and Pt–Ru alloys prepared with different amounts of reducing agent showing the location of absent hcp Ru and Ru-oxide peaks.

EDS analysis further confirmed the successful incorporation of Ru into the alloy phase with a Pt:Ru atomic ratio of 70.5:29.5 determined for the Pt–Ru 0.4 g materials. No characteristic peaks of hexagonal Ru or oxide species were detected in the whole range of XRD patterns, commonly reported for PtRu alloys with similar compositions [11]. This indicates that Ru atoms are incorporated into the fcc Pt lattice forming a well dispersed alloy. This results in a decrease of the lattice parameter and the Pt–Pt interatomic distances observed due to the smaller radius of the Ru atoms compared with Pt.

Fig. 2 presents TEM images of the Pt–Ru materials synthesized using different reducing agent amounts. As shown in Fig. 2b, well developed Pt–Ru NWNs were successfully synthesized using the soft template procedure and 0.4 g of $NaBH_4$ reducing agent. The Pt–Ru nanowires are seen to interconnect to form two-dimensional (2D) NWNs. The nanowires have an average cross-sectional diameter of 3.0 ± 0.5 nm and the distribution of the NWNs is very uniform. The polycrystalline interconnected nanowires of the Pt–Ru NWNs can be clearly observed from the high resolution TEM (HRTEM) image in Fig. 2d. The lattice spacing of the alloy nanowires is measured as 2.22 Å, slightly less than that from the (111) diffraction of the fcc phase of platinum (2.26 Å) [12]. Interestingly, by varying the amount of reducing agent added, it was found that the distinct nanostructures of Pt–Ru can be somewhat altered. By varying the amount of reducing agent from 0.2 g to 0.6 g, the Pt–Ru nanostructures evolved as shown in the TEM images of Fig. 2. Pt–Ru NWN formation was found to be favored at the optimal addition of 0.4 g of reducing agent. Fig. 2 also illustrates the possible formation process of Pt–Ru nanostructures highlighting the effect of the amount of reducing agent. This schematic demonstrates the unique, dynamic self-assembly of CTAB into worm-like micelles in a water–chloroform mixture due to the hydrophobic/hydrophilic interactions occurring between the surfactant molecules at the two-phase interface. Pt and Ru containing ions present in the aqueous phase can then be drawn into the worm-like micelles most likely due to the distinct hydrophobic interactions occurring at the water/chloroform interface and the electrostatic interactions occurring between metal ions with each other or with the hydrophilic head of the CTAB molecules [13]. Addition of a $NaBH_4$ reducing agent will then allow the reduction of these metal ions into metallic nanostructures templated by the self-assembled aggregate structures. In general, if the amount of reducing agent added is too low, for example 0.2 g, aggregated Pt–Ru nanoparticles are formed as observed in Fig. 2a and e, due to the fact that the Pt and Ru precursors were not completely reduced. If the amount of reducing agent added is too high, for example 0.6 g, the Pt–Ru also appears as nanoparticles as observed in Fig. 2c and g, due to the fact

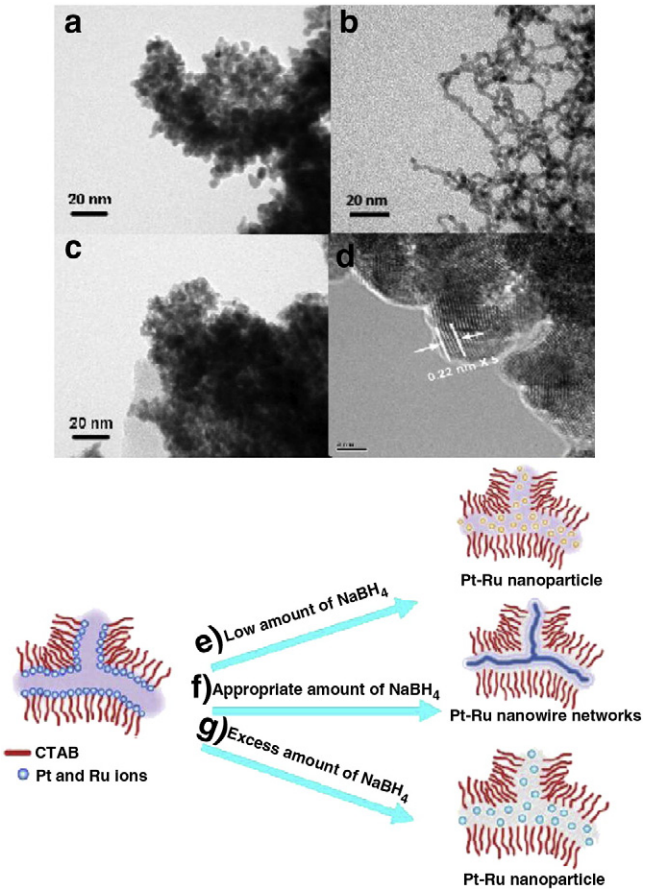

Fig. 2. TEM images of Pt–Ru alloy catalysts prepared with different amounts of reducing agent, a, 0.2 g (Pt–Ru 0.2 g); b, 0.4 g (Pt–Ru 0.4 g); and c, 0.6 g (Pt–Ru 0.6 g); d, high resolution TEM image of Pt–Ru NWNs (Pt–Ru 0.4 g), and e, f and g are a schematic illustrating the effect of reducing agent on Pt–Ru nanostructures.

that the Pt and Ru precursors were reduced too rapidly and the CTAB did not act as a soft template. When the amount of reducing agent was 0.4 g (Fig. 2b and f), the Pt–Ru formed relatively uniform NWNs. These observations are supported by the XRD patterns provide in Fig. 1, where higher intensity diffraction peaks are observed for 0.4 g of reducing agent due to the formation of well defined interconnected crystalline structures, whereas reduced intensity, broadened peaks are observed for 0.2 and 0.6 g due to the small aggregated nanoparticles formed.

3.2. Electrochemical testing

The effect of varying the amount of reducing agent was investigated on the electrocatalytic activity of Pt–Ru toward the MOR as displayed in Fig. 3. The forward peak current density (I_f) in the anodic direction can be regarded as methanol oxidation on non-poisoned catalysts, whereas the backward peak current density in the cathodic direction is associated with oxidation and removal of the carbonaceous intermediate species [14]. It can be clearly seen that when the amount of reducing agent is 0.4 g, Pt–Ru NWNs possess the highest MOR activity compared to other Pt–Ru catalysts prepared at 0.2 g and 0.6 g, respectively. In order to attribute the observed oxidation current at higher electrode potentials to the MOR, CV was carried out in 0.1 M $HClO_4$ electrolyte in the absence of methanol reactant. The inset of Fig. 3 demonstrates the CV curve obtained for Pt–Ru 0.4 g and confirms that the high oxidation currents observed for these materials in methanol containing electrolyte are due to the MOR.

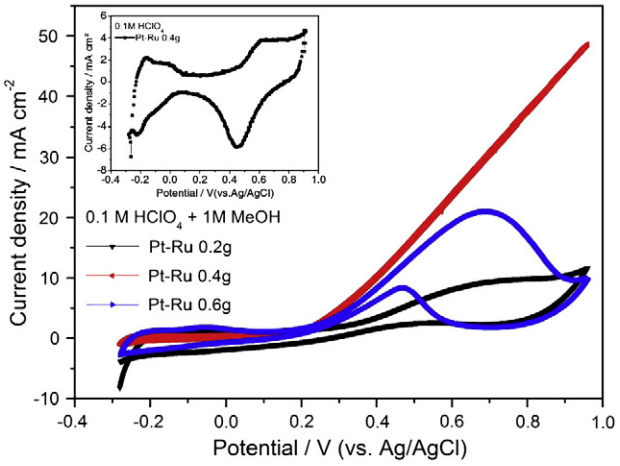

Fig. 3. Cyclic voltammograms of as-prepared Pt–Ru at different amounts of reducing agent for MOR, (inset) cyclic voltammogram of Pt–Ru 0.4 g in the same electrolyte in the absence of methanol.

The effect of varying the atomic ratios of Pt and Ru in the precursor solutions while maintaining constant reducing agent amounts (0.4 g) was also investigated for MOR as displayed in Fig. 4. From Fig. 4 it can be seen that when the atomic ratio of Pt and Ru precursors is 1:1, the Pt–Ru catalysts possess the highest I_f, indicating the best electrocatalytic activity toward the MOR. However, when the content of Ru in the Pt–Ru catalyst is too high, the electrocatalytic activity of the Pt–Ru NWNs catalyst would decrease. Therefore, an optimal atomic ratio of 1:1 has been determined to provide the highest MOR activity.

Fig. 5 shows the MOR specific activity of Pt–Ru NWNs compared to commercial Pt black, 20% Pt/C and Pt–Ru black. It can be seen clearly that Pt–Ru NWNs possess the highest MOR activity at 0.7 V vs Ag/AgCl compared to commercial Pt black, 20% Pt/C and Pt–Ru black in the forward scan direction. The current densities obtained from CV at 0.7 V vs Ag/AgCl are 30.95 mA cm^{-2} for Pt–Ru NWNs, superior to that of 23.5 mA cm^{-2} for Pt–Ru black, which is the best catalyst for MOR and CO tolerance to date. Both these materials provided significant improvements over Pt black and Pt/C, displaying current densities of 2.0 mA cm^{-2} and 18.8 mA cm^{-2}, respectively. In addition, no oxidation peaks of carbonaceous intermediates on the Pt–Ru NWN electrode are seen in the backward scan direction, which indicates exceptional CO tolerance. This CO tolerance primarily results from the oxygen

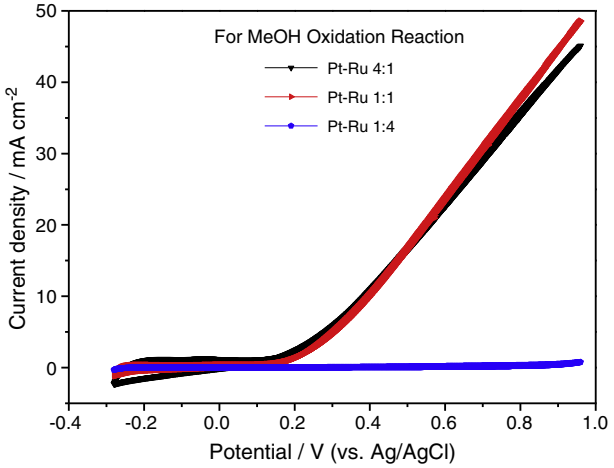

Fig. 4. Cyclic voltammograms of as-prepared Pt–Ru at different precursor atomic ratios of Pt and Ru for MOR.

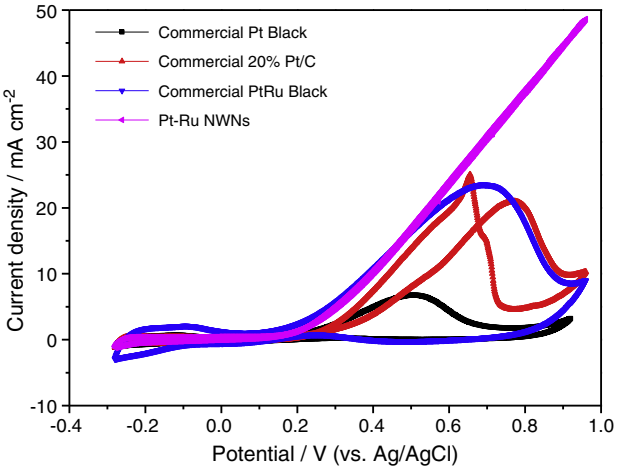

Fig. 5. Cyclic voltammograms of commercial Pt black, commercial 20% Pt/C, commercial Pt–Ru black and as-prepared Pt–Ru NWNs for the MOR.

containing groups present on Ru sites which can facilitate the oxidation of adsorbed CO species on adjacent Pt active sites, a phenomena that has been discussed elsewhere [8,9]. The high activity of Pt–Ru NWNs is most likely due to the interconnected, polycrystalline structure of Pt–Ru NWN catalysts containing a large number of electronically connected catalytically active sites available for reactant access. This in turn facilitated the strong adsorption and activation of methanol molecules on the surface of Pt–Ru NWNs and hence, the enhancement of the electrocatalytic activity of Pt–Ru NWNs for the MOR. On the other hand, the Pt modified by Ru leads to lattice contraction (by XRD) which can also play a role in determining the catalytic activities. We conclude that the Pt–Ru NWNs can be considered a promising replacement to commercial Pt–Ru as an anode catalyst material for DMFCs.

4. Conclusions

In summary, Pt–Ru NWNs have been successfully synthesized by a simple soft template procedure for use as MOR electrocatalysts for fuel cell applications. Synthesis conditions, such as the amount of reducing agent and the atomic ratios of Pt and Ru, were found to significantly affect the activity of Pt–Ru NWN electrocatalysts. These 2D Pt–Ru NWNs demonstrated significant MOR activity and CO tolerance through half-cell testing, superior to that of commercially available Pt–Ru black. Thus, Pt–Ru NWNs are presented as highly active electrocatalyst materials for potential replacement of the commercial Pt–Ru as anode catalysts for DMFC applications.

Acknowledgements

This work was funded by Natural Sciences and Engineering Research Council of Canada (NSERC) and the University of Waterloo.

References

[1] H. Liu, C. Song, L. Zhang, J.J. Zhang, H.J. Wang, D.P. Wilkinson, Journal of Power Sources 155 (2006) 95–110.
[2] K. Lee, L. Zhang, J.J. Zhang, Journal of Power Sources 165 (2007) 108–113.
[3] C. Lamy, J.M. Leger, S. Srinivasan, B.E. Conway, R.E. White (Eds.), Modern Aspects of Electrochemistry, 34 (2001) 53–118.
[4] Y.S. Kim, B.S. Pivovar, Advances in Fuel Cells 1 (2007) 187–234.
[5] Z.W. Chen, M. Waje, W.Z. Li, Y.S. Yan, Angewandte Chemie, International Edition 46 (2007) 4060–4063.
[6] V.R. Stamenkovic, B. Fowler, B.S. Mun, G.F. Wang, P.N. Ross, C.A. Lucas, N.M. Markovic, Science 315 (2007) 493–497.
[7] Z.M. Peng, H. Yang, Journal of the American Chemical Society 131 (2009) 7542–7543.
[8] K. Koczkur, Q.F. Yi, A.C. Chen, Advanced Materials 19 (2007) 2648–2652.
[9] W.C. Choi, S.I. Woo, Journal of Power Sources 124 (2003) 420–425.
[10] S.Y. Wang, S.P. Jiang, X. Wang, J. Guo, Electrochimica Acta 56 (2011) 1563–1569.
[11] X. Zhang, K.Y. Chan, Chemistry of Materials 15 (2003) 451–459.
[12] S.C. Yang, F. Hong, L.Q. Wang, S.W. Guo, X.P. Song, B.J. Ding, Z.M. Yang, Journal of Physical Chemistry C 114 (2010) 203–207.
[13] Y. Song, R.M. Garcia, R.M. Dorin, H. Wang, Y. Qiu, E. Coker, W. Steen, J. Miller, J. Shelnutt, Nano Letters 7 (2007) 3650–3655.
[14] J. Prabhuram, R. Manoharan, Journal of Power Sources 74 (1998) 54–61.